

# Search for three-nucleon short-range correlations in nuclei

Z. Ye,<sup>1,2</sup> P. Solvignon,<sup>3,4</sup> J. Arrington,<sup>5</sup> D. Day,<sup>1</sup> D. W. Higinbotham,<sup>3</sup> P. Aguilera,<sup>6</sup> Z. Ahmed,<sup>7</sup> H. Albataineh,<sup>8</sup> K. Allada,<sup>9</sup> B. Anderson,<sup>10</sup> D. Anez,<sup>11</sup> K. Aniol,<sup>12</sup> J. Annand,<sup>13</sup> W. Armstrong,<sup>14</sup> T. Averett,<sup>15</sup> T. Badman,<sup>4</sup> H. Baghdasaryan,<sup>1</sup> X. Bai,<sup>16</sup> A. Beck,<sup>17</sup> S. Beck,<sup>17</sup> V. Bellini,<sup>18</sup> F. Benmokhtar,<sup>19</sup> W. Bertozzi,<sup>20</sup> J. Bittner,<sup>21</sup> W. Boeglin,<sup>22</sup> A. Camsonne,<sup>3</sup> C. Chen,<sup>23</sup> J.-P. Chen,<sup>3</sup> K. Chirapatpimol,<sup>1</sup> E. Cisbani,<sup>24</sup> M. M. Dalton,<sup>1</sup> A. Daniel,<sup>25</sup> C. W. de Jager,<sup>3,1</sup> R. De Leo,<sup>26</sup> W. Deconinck,<sup>20</sup> M. Defurne,<sup>27</sup> D. Flay,<sup>14</sup> N. Fomin,<sup>28</sup> M. Friend,<sup>19</sup> S. Frullani,<sup>24</sup> E. Fuchey,<sup>14</sup> F. Garibaldi,<sup>24</sup> D. Gaskell,<sup>3</sup> S. Gilad,<sup>20</sup> R. Gilman,<sup>29,3</sup> O. Glamazdin,<sup>30</sup> C. Gu,<sup>1</sup> P. Gueye,<sup>23</sup> D. Hamilton,<sup>13</sup> C. Hanretty,<sup>31</sup> J.-O. Hansen,<sup>3</sup> M. Hashemi Shabestari,<sup>1</sup> O. Hen,<sup>32</sup> T. Holmstrom,<sup>21</sup> M. Huang,<sup>2</sup> S. Iqbal,<sup>12</sup> G. Jin,<sup>1</sup> N. Kalantarians,<sup>33</sup> H. Kang,<sup>34</sup> A. Kelleher,<sup>20</sup> M. Khandaker,<sup>35</sup> I. Korover,<sup>32</sup> J. LeRose,<sup>3</sup> J. Leckey,<sup>36</sup> R. Lindgren,<sup>1</sup> E. Long,<sup>4</sup> J. Mammei,<sup>37</sup> D. J. Margaziotis,<sup>12</sup> P. Markowitz,<sup>22</sup> A. Marti Jimenez-Arguello,<sup>38</sup> D. Meekins,<sup>3</sup> Z. Meziani,<sup>14</sup> R. Michaels,<sup>3</sup> M. Mihovilovic,<sup>39</sup> P. Monaghan,<sup>20</sup> N. Muangma,<sup>20,23</sup> C. Munoz Camacho,<sup>38</sup> B. Norum,<sup>1</sup> Nuruzzaman,<sup>40</sup> K. Pan,<sup>20</sup> S. Phillips,<sup>4</sup> E. Piasetzky,<sup>32</sup> I. Pomerantz,<sup>32,41</sup> M. Posik,<sup>14</sup> V. Punjabi,<sup>35</sup> X. Qian,<sup>2</sup> Y. Qiang,<sup>2</sup> X. Qiu,<sup>42</sup> P. E. Reimer,<sup>5</sup> A. Rakhman,<sup>7</sup> S. Riordan,<sup>1,43</sup> G. Ron,<sup>44</sup> O. Rondon-Aramayo,<sup>1</sup> A. Saha,<sup>3,\*</sup> E. Schulte,<sup>29</sup> L. Selvy,<sup>10</sup> A. Shahinyan,<sup>45</sup> R. Shneur,<sup>32</sup> S. Sirca,<sup>46</sup> J. Sjoegren,<sup>13</sup> K. Slifer,<sup>4</sup> N. Sparveris,<sup>14</sup> R. Subedi,<sup>1</sup> V. Sulkosky,<sup>20,21</sup> W. Tireman,<sup>47</sup> D. Wang,<sup>1</sup> J. W. Watson,<sup>10</sup> L. B. Weinstein,<sup>8</sup> B. Wojtsekhowski,<sup>3</sup> S. A. Wood,<sup>3</sup> W. Yan,<sup>48</sup> I. Yaron,<sup>32</sup> X. Zhan,<sup>5</sup> J. Zhang,<sup>3</sup> Y. Zhang,<sup>29</sup> B. Zhao,<sup>15</sup> Z. Zhao,<sup>1</sup> X. Zheng,<sup>1</sup> P. Zhu,<sup>48</sup> and R. Zielinski<sup>4</sup>

(The Jefferson Lab Hall A Collaboration)

<sup>1</sup>University of Virginia, Charlottesville, VA 22904

<sup>2</sup>Duke University, Durham, NC 27708

<sup>3</sup>Thomas Jefferson National Accelerator Facility, Newport News, VA 23606

<sup>4</sup>University of New Hampshire, Durham, NH 03824

<sup>5</sup>Physics Division, Argonne National Laboratory, Argonne, IL 60439

<sup>6</sup>Institut de Physique Nucléaire (UMR 8608), CNRS/IN2P3 - Université Paris-Sud, F-91406 Orsay Cedex, France

<sup>7</sup>Syracuse University, Syracuse, NY 13244

<sup>8</sup>Old Dominion University, Norfolk, VA 23529

<sup>9</sup>University of Kentucky, Lexington, KY 40506

<sup>10</sup>Kent State University, Kent, OH 44242

<sup>11</sup>Saint Mary's University, Halifax, Nova Scotia, Canada

<sup>12</sup>California State University, Los Angeles, Los Angeles, CA 90032

<sup>13</sup>University of Glasgow, Glasgow G12 8QQ, Scotland, United Kingdom

<sup>14</sup>Temple University, Philadelphia, PA 19122

<sup>15</sup>College of William and Mary, Williamsburg, VA 23187

<sup>16</sup>China Institute of Atomic Energy, Beijing, China

<sup>17</sup>Nuclear Research Center Negev, Beer-Sheva, Israel

<sup>18</sup>Universita di Catania, Catania, Italy

<sup>19</sup>Carnegie Mellon University, Pittsburgh, PA 15213

<sup>20</sup>Massachusetts Institute of Technology, Cambridge, MA 02139

<sup>21</sup>Longwood University, Farmville, VA 23909

<sup>22</sup>Florida International University, Miami, FL 33199

<sup>23</sup>Hampton University, Hampton, VA 23668

<sup>24</sup>INFN, Sezione Sanità and Istituto Superiore di Sanità, 00161 Rome, Italy

<sup>25</sup>Ohio University, Athens, OH 45701

<sup>26</sup>INFN, Sezione di Bari and University of Bari, I-70126 Bari, Italy

<sup>27</sup>CEA Saclay, F-91191 Gif-sur-Yvette, France

<sup>28</sup>University of Tennessee, Knoxville, TN 37996

<sup>29</sup>Rutgers, The State University of New Jersey, Piscataway, NJ 08855

<sup>30</sup>Kharkov Institute of Physics and Technology, Kharkov 61108, Ukraine

<sup>31</sup>Florida State University, Tallahassee, FL 32306

<sup>32</sup>Tel Aviv University, Tel Aviv 69978, Israel

<sup>33</sup>University of Texas, Houston, TX 77030

<sup>34</sup>Seoul National University, Seoul, Korea

<sup>35</sup>Norfolk State University, Norfolk, VA 23504

<sup>36</sup>Indiana University, Bloomington, IN 47405

<sup>37</sup>Virginia Polytechnic Inst. and State Univ., Blacksburg, VA 24061

<sup>38</sup>Université Blaise Pascal/IN2P3, F-63177 Aubière, France

<sup>39</sup>Jozef Stefan Institute, Ljubljana, Slovenia

<sup>40</sup>Mississippi State University, Mississippi State, MS 39762

<sup>41</sup>*The University of Texas at Austin, Austin, Texas 78712*

<sup>42</sup>*Lanzhou University, Lanzhou, China*

<sup>43</sup>*University of Massachusetts, Amherst, MA 01006*

<sup>44</sup>*Racah Institute of Physics, Hebrew University of Jerusalem, Jerusalem, Israel*

<sup>45</sup>*Yerevan Physics Institute, Yerevan 375036, Armenia*

<sup>46</sup>*University of Ljubljana, Ljubljana, Slovenia*

<sup>47</sup>*Northern Michigan University, Marquette, MI 49855*

<sup>48</sup>*University of Science and Technology, Hefei, China*

(Dated: July 13, 2015)

We present new data probing short-range correlations (SRC) in nuclei through the measurement of electron scattering off high-momentum nucleons in light nuclei. The inclusive cross section ratios of  $^4\text{He}$  to  $^3\text{He}$  and  $^{12}\text{C}$  to  $^3\text{He}$  are observed to be both  $Q^2$  and  $x$  independent for  $1.5 < x < 2$ , confirming the previously observed dominance of two-nucleon short-range corrections. We also examine the  $Q^2$  dependence for  $x > 2$  where previous data suggested that scattering from three-nucleon correlations might dominate the cross section.

PACS numbers: 25.10.1s, 25.30.Fj

Understanding the complex structure of nuclei remains one of the major tasks in nuclear physics, and several questions remain about the high-momentum components of the nuclear wavefunction. This is an important component of nuclear structure that goes beyond the shell model description. Mean field calculations [1] do not include these high-momentum components, and so significantly overpredict the cross section for proton knockout reactions with proton momenta below the Fermi momenta [2, 3, 4]

In the dense and energetic environment of the nucleus, nucleons have a significant probability of interacting at distance near or below 1 fm, even in light nuclei [5, 6]. Protons and neutrons interacting through the strong, short-distance components of the NN potential yield pairs of nucleons with large momenta, well above the typical scale of the Fermi momentum associated with the shell model picture of nuclei. These pairs of high-momentum nucleons, the so-called short-range correlations (SRCs), are the dominant source of the high-momentum part of the nuclear momentum distribution [7, 8]. Thus, the nuclear momentum distribution has two distinct regions, driven by very different physics. For momenta below the Fermi momentum,  $k_F \approx 300$  MeV/c, we have collective, shell-model behavior which varies rapidly with  $A$ . For momenta above  $k_F$ , two-body physics dominates and there is a universal structure for all nuclei, driven by the details of the two-body NN interaction [9, 10, 11].

Because the momentum distribution of the nucleus is not an experimental observable, one cannot simply measure this for all nuclei and compare the high-momentum components. One can, however, test the idea of a universal structure to the high-momentum components by comparing quasi-elastic scattering from different nuclei at kinematics which require that the struck nucleon have a large initial momentum [10]. During the scattering, the electron transfers energy,  $\nu$ , and momentum  $\vec{q}$  to the struck nucleon by exchanging a virtual photon with

four momentum transfer  $q^2 = -Q^2 = \nu^2 - |\vec{q}|^2$ . It is useful in this case to define the kinematic variable  $x = Q^2/(2M_p\nu)$ , where  $M_p$  is the mass of the proton. Elastic scattering from a stationary proton corresponds to  $x = 1$ , while  $x > 1$  corresponds to high momentum transfer but low energy transfer. This requires that the virtual photon be absorbed by a proton whose initial momentum is opposite to the momentum of the virtual photon, so that the large transferred momentum changes the direction of the proton's momentum while minimizing the magnitude of the final momentum and thus the proton's kinetic energy. Scattering at  $x > 1$  must involve more than one nucleon as the initial momentum of the struck nucleon must be balanced by one or more nucleons in the nucleus. The kinematic limit for scattering from a nucleus is  $x = M_A/M_p \approx A$ , which for scattering from the deuteron corresponds to  $x \approx 2$ ; scattering at  $x > 2$  thus involves the participation of at least three nucleons.

Based on these kinematic arguments, one can use  $x$  to determine the minimum number of nucleons involved in the interaction. Values of  $x$  slightly greater than unity requires only a small momentum which can come from either the single-particle contributions or from high-momentum nucleons associated with SRCs. As  $x$  increases, larger momenta are required and for sufficiently large  $x$  scattering from nucleons below the Fermi momentum is forbidden, isolating scattering from SRCs [9, 10]. Previous measurements at SLAC and Jefferson Lab revealed a universal form to the high-momentum distributions of the struck nucleons [7, 8, 12, 13, 14]. In these experiments, the ratio of scattering from a heavy nucleus to the deuteron was shown to scale, i.e. be independent of  $x$  and  $Q^2$ , for  $x \gtrsim 1.5$  and  $Q^2 \gtrsim 1.5$  GeV<sup>2</sup>, corresponding to scattering from nucleons with momenta above 300 MeV/c. Other measurements have demonstrated that these high-momentum components are dominated by high-momentum n-p pairs [15, 16, 17], meaning that the high-momentum components in all nuclei have a deuteron-like structure.

Taking ratios of heavier nuclei to  $^3\text{He}$  allows a similar examination of the target ratios for  $x > 2$ , where one might expect to see a universal signature of three-nucleon SRCs - configurations of three nucleons which have large relative but small total momenta. These configurations could come from either three-nucleon forces or successive hard two-nucleon interactions. The first such measurement [12] observed ratios which were independent of  $x$  above  $x = 2.25$ , and this was taken as an indication that the 3N-SRCs dominated in this region and extracted the relative contribution of the 3N-SRCs in heavy nuclei compared to  $^3\text{He}$ . However the ratios were measured at relatively low  $Q^2$  and the  $Q^2$  dependence was not measured. A later experiment [14] at higher  $Q^2$  yielded  $^4\text{He}/^3\text{He}$  ratios that were significantly larger than those from [12]. Thus the question of whether 3N-SRC contributions have been cleanly identified and observed to dominate at some very large momentum scale is as yet unanswered.

The results reported here are from JLab experiment E08-014 [18], carried out in Hall A and focused on precise measurements of the  $x$  and  $Q^2$  dependence of the  $A/^3\text{He}$  cross section ratio at large  $x$ . An electron beam with an energy of 3.356 GeV and currents ranging from XX to YY  $\mu\text{A}$  impinged on nuclear targets and the scattered electrons were detected in two nearly identical High-Resolution Spectrometers (HRSs) [19]. Three 20 cm cryogenic targets were used, liquid  $^2\text{H}$  and gaseous  $^3\text{He}$  and  $^4\text{He}$ , along with thin foils of  $^{12}\text{C}$ ,  $^{40}\text{Ca}$  and  $^{48}\text{Ca}$ . Each HRS consists of a pair of vertical drift chambers (VDCs) for particle tracking, two scintillator planes for triggering and timing measurements, and a gas Čerenkov counter and two layers of lead-glass calorimeters for particle identification [19]. Scattering was measured at  $\theta_0 = 21^\circ, 23^\circ, 25^\circ$ , and  $28^\circ$ , cover a  $Q^2$  range of 1.3–2.2  $\text{GeV}^2$ . A detailed description of the experiment and data analysis can be found in Ref. [20].

The analysis keeps events where a single track is identified, with very small corrections for multi-track events as the event rates are modest for the large- $x$  kinematics. The trigger and tracking inefficiencies are extremely small and applied as a correction to the measured yield. Electrons are identified by applying cuts on the signals from both the Čerenkov detector and the calorimeters. The cuts yield  $> 99\%$  electron efficiency with negligible pion contamination. The overall dead-time of the data acquisition system (DAQ) was evaluated run-by-run and this correction was applied to the measured yield.

The scattered electron momentum, in-plane and out-of-plane angles, and vertex position at the target can be reconstructed with the optics matrices of the HRSs using the tracking information from the VDCs as inputs. The optics matrices have been well calibrated by previous experiments and were also optimized with the new calibration data taken during this experiment. To reduce the edge effects due to the spectrometers' geometries, only the central acceptance regions were chose by cut-

ting on these reconstructed quantities. A Monte Carlo (MC) simulation of the HRSs [20] was used to correct for the residual acceptance effect. *JRA: Probably need to at least mention modified tune/optics of right arm. We'll probably refer to it in context of check of left arm data, even if we don't use it. I assume that the plan is to show left arm only, as we don't need optimal statistics in this case..*

For the cryogenic targets, we exclude events which come from scattering in the cell walls by applying a cut on the reconstructed vertex position of the scattered electron on the target. A dummy target of two thin aluminum foils with 20 cm apart was used to evaluate the level of residual endcap contribution after the cut. We apply a cut  $\pm 7$  cm around the center of the target target, removing  $> 99.9\%$  of the events from target endcap scattering. One of the largest sources of systematic uncertainty comes from target density reduction due to heating of the  $^2\text{H}$ ,  $^3\text{He}$ , and  $^4\text{He}$  targets in the high-current electron beam. We made dedicated measurements varying beam currents and used the variation of the yield to measure the current dependence of the target density. This was used to determine the effective target length at the current of the measurement. We assigned a conservative uncertainty of 5% on the target density for each cryogenic target.

(FIX-HERE: Discuss more about the dominant systematic uncertainties).

The measured events, corrected for inefficiencies and normalized to the integrated luminosity, were binned in  $x$  and compared to the simulated yield. The simulation uses a  $y$ -scaling cross section model with radiative corrections applied using the peaking approximation [20]. *JRA: Probably want reference to paper with RC formalism used.* For each  $x$  bin, the ratio of experimental to Monte Carlo yield is applied as a correction to the cross section model at that  $x$  value to extract the cross section.

*JRA: How large are Coulomb corrections if we (a) exclude or (b) include Calcium?*

The absolute cross sections for scattering from  $^3\text{He}$ ,  $^4\text{He}$  and  $^{12}\text{C}$  at a scattering angle of  $25^\circ$  are shown in Fig. 1.

Fig. 2 presents the ratio of the  $^4\text{He}$  and  $^{12}\text{C}$  cross sections to  $^3\text{He}$  as a function of  $x$ . In the 2N-SRC region, our data are in good agreement with the data from CLAS [12] and E02-019 [14], revealing a plateau between  $x \approx 1.5$  and  $x = 2$ . At  $x > 2$ , our ratios are significantly larger than the CLAS ratios, and in generally good agreement with the E02-019 ratios. The disagreement between the CLAS ratios and both our results and the E02-019 data suggest a problem with the extracted ratios from Ref. [12] above  $x = 2$ . A recent comment [21] suggested that the 3N-SRC plateau showed in the CLAS data could be a result of inappropriate binning and bin-centering correction.

We observe a small but systematic  $Q^2$  dependence in

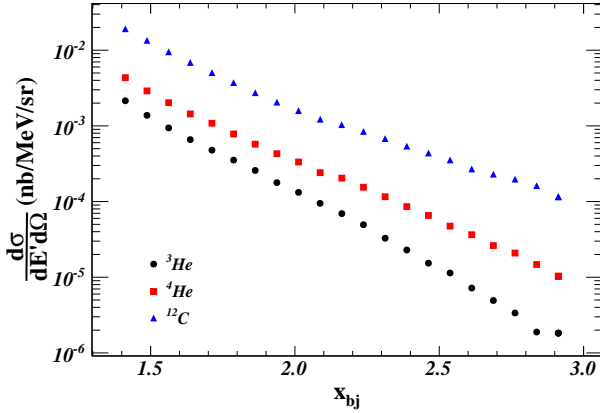


FIG. 1. (Color online) Cross sections of  $^3\text{He}$ ,  $^4\text{He}$  and  $^{12}\text{C}$  at  $25^\circ$ . The uncertainties include statistical and systematic uncertainties. An additional normalization uncertainty of XX% is not shown.

our data, and do not see indications of a well defined 3N-SRC plateau. Instead our ratios show a slow rise above  $x = 2$ , with a more rapid increase as  $x \rightarrow 3$ , suggesting that the simple model of 3N-SRC dominance is not valid in this region. While this behavior does not match the prediction of the native 3N-SRC model, namely  $A/^3\text{He}$  ratios independent of  $x$  and  $Q^2$  for  $x \gtrsim 2.5$ , this does not provide a clear demonstration that 3N-SRCs are unimportant in this region.

For 2N-SRCs, the prediction of scaling is relatively straightforward and robust. One can predict *a priori* where the plateau should be observed since for any given  $Q^2$ , a value of  $x$  can be selected that corresponds to a minimum nucleon momentum that is above the Fermi momentum, thus suppressing the mean-field contributions. As one approaches  $x = 2$ , the plateau will disappear as the deuteron cross section falls to zero and so the  $A/^2\text{H}$  ratios must rise sharply to infinity. For both the data and our simple cross section model, based on a calculated deuteron momentum distribution, this does not occur until  $x \approx 1.9$ , yielding a clear plateau for  $1.5 < x < 1.9$ .

In attempting to isolate 3N-SRC contributions, the situation is less straightforward. Both 2N and 3N SRCs yield contributions to the high-momentum tail. The fact that we do not see significant deviations from the 2N-SRC picture for  $1.5 < x < 2$  suggests that the 3N-SRC contributions are generally much smaller. Unlike the case for 2N-SRCs, where  $k > k_F$  suppresses single particle strength, there is not a clear way to define a threshold in  $x$  that will sufficiently suppress 2N contributions. Approaching the kinematic limit at  $x \approx 3$ , the  $^3\text{He}$  cross section falls to zero and the ratio must go to infinity. However, while this occurs in a vary narrow  $x$  window for the  $A/^2\text{H}$  ratios, the rise occurs over a larger range

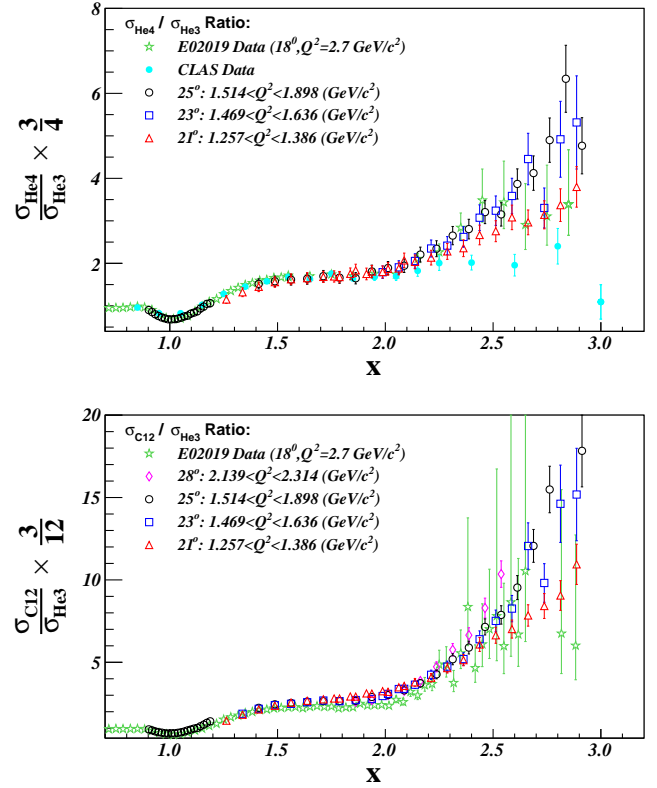


FIG. 2. (Color online) The  $^4\text{He}/^3\text{He}$  (top) and  $^{12}\text{C}/^3\text{He}$  (bottom) cross section ratios for this measurement, along with results from CLAS [12] and Hall C (E02-019) [14] measurements. Uncertainties include statistical and systematic uncertainties. A normalization uncertainty of XX% (top) and YY% (bottom) is not included. *JRA: It will be good to make these large, so making the y-axis labels less 'tall' will help, e.g. something like  $(\sigma_{4\text{He}}/4)/(\sigma_{3\text{He}}/3)$ . Do we want to include our cross section model to show  $Q^2$  dependence?*

in  $x$  in this case.

Thus, it is not clear that there will be a significant window in  $x$  where one would expect to see a plateau, especially at the relatively modest  $Q^2$  values measured here. In the present experiment, we observe a small but noticeable  $Q^2$  dependence, in particular for  $x \gtrsim 2.5$ . This is also observed in our simple  $y$ -scaling cross section model, and does not occur in the  $^{12}\text{C}/^3\text{He}$  ratio, indicating that it is the  $x$  dependence of the falloff of the  $^3\text{He}$  cross section as  $x \rightarrow 3$  that is varying strongly with  $Q^2$ . Larger  $Q^2$  values may be required to observe a  $Q^2$ -independent behavior of the ratios with  $x$ , which may allow us to isolate 3N-SRC contributions.

Figure with  $A/2\text{H}$  ratios up to  $x = 2$ , table with  $a_2$  results for  $A = 3, 4, 12, 48$ ?

(Add conclusion here). Also, brief discussion of future experiments (certainly  $x > 1$  in Hall C, probably  $x < 3$  in Hall A as well).

We would like to acknowledge the outstanding sup-

port from the Jefferson Lab Hall A technical staff and  
the JLab target group. This work was supported by the  
NSF and the DOE, Office of Science, Office of Nuclear  
Physics, under contract DE-AC02-06CH11357, and by  
DOE contract DE-AC05-06OR23177 under which JSA,  
LLC operates JLab.

---

\* deceased

- [1] J. D. Forest, Nucl. Phys. **A392**, 232 (1983).
- [2] G. V. D. Steenhoven *et al.*, Nucl. Phys. A **480**, 547 (1988).
- [3] L. Lapiks, Nucl. Phys. A **553**, 297 (1993).
- [4] J. Kelly, Adv. Nucl. Phys. **23**, 75 (1996).
- [5] J. Carlson *et al.*, (2014), 1412.3081.
- [6] Z. T. Lu *et al.*, Rev. Mod. Phys. **85**, 1383 (2013).
- [7] J. Arrington, D. Higinbotham, G. Rosner, and M. Sargsian, Prog. Part. Nucl. Phys. **67**, 898 (2012).
- [8] L. L. Frankfurt, M. I. Strikman, D. B. Day, and M. Sargsyan, Phys. Rev. C **48**, 2451 (1993).
- [9] C. Ciofi degli Atti and S. Simula, Phys. Rev. C **53**, 1689 (1996).
- [10] O. Benhar, D. Day, and I. Sick, Rev. Mod. Phys. **80**, 189 (2008).
- [11] R. Wiringa, R. Schiavilla, S. C. Pieper, and J. Carlson, Phys. Rev. **C89**, 024305 (2014).
- [12] K. S. Egiyan *et al.*, Phys. Rev. Lett. **96**, 082501 (2006).
- [13] K. Egiyan *et al.*, Phys. Rev. **C68**, 014313.
- [14] N. Fomin *et al.*, Phys. Rev. Lett. **108**, 092502 (2012).
- [15] R. Subedi *et al.*, Science **320**, 1476 (2008).
- [16] I. Korover *et al.*, Phys. Rev. Lett. **113**, 022501 (2014).
- [17] O. Hen *et al.*, Science **346**, 614 (2014).
- [18] J. Arrington, D. Day, D. Higinbotham, and P. Solvignon, Three-nucleon short range correlations studies in inclusive scattering for  $0.8 < Q^2 < 2.8(\text{GeV}/c)^2$ , <http://hallaweb.jlab.org/experiment/E08-014/>, 2011.
- [19] J. Alcorn *et al.*, Nucl. Instrum. Meth. **A522**, 294 (2004).
- [20] Z. Ye, Ph.D Thesis, University of Virginia, 2013, arXiv:1408.5861.
- [21] D. W. Higinbotham and O. Hen, Phys. Rev. Lett. **114**, 169201 (2015).